Vortex pinning properties in Fe-chalcogenides

A Leo[1,2], G Grimaldi[2], A Guarino[1,2], F Avitabile[1], A Nigro[1,2], A Galluzzi[1], D Mancusi[1], M Polichetti[1,2], S Pace[1,2], K Buchkov[3], E Nazarova[3], S Kawale[4], E Bellingeri[4], C Ferdeghini[4]

[1] Dipartimento di Fisica "E. R. Caianiello", Universitá di Salerno, via Giovanni Paolo II, 132, I-84084 Fisciano (SA), Italy
[2] CNR-SPIN Salerno, via Giovanni Paolo II, 132, I-84084 Fisciano (SA), Italy
[3] "Georgi Nadjakov"Institute of Solid State Physics, Bulgarian Academy of Sciences, 72 Tsarigradsko shosse Blvd., 1784 Sofia, Bulgaria
[4] CNR-SPIN Genova, corso Perrone, 24, I-16152 Genova, Italy

E-mail: antoleo@sa.infn.it

Abstract. Among the families of iron-based superconductors, the 11-family is one of the most attractive for high field applications at low temperatures. The optimization of the fabrication processes for bulk, crystalline and/or thin film samples is the first step for producing wires and/or tapes for practical high power conductors. Here we present the results of a comparative study of the pinning properties in iron-chalcogenides, investigating the flux pinning mechanisms in optimized $Fe(Se_{1-x}Te_x)$ and FeSe samples by current-voltage characterizations, magneto-resistance and magnetization measurements. In particular, from the Arrhenius plots in the magnetic fields up to 9 T, the activation energy is derived as a function of magnetic field, $U_0(H)$, whereas the activation energy as a function of temperature, $U(T)$, is derived from relaxation magnetization curves. The high pinning energies, high upper critical field vs. temperature slopes near critical temperature and highly isotropic pinning properties, can candidate the iron-chalcogenide superconductors to be a technological material which could be a real competitor of cuprate high temperature superconductors for high field applications.

Keywords: Fe-based superconductors, flux pinning, high-temperature superconductors, superconducting materials, superconducting transition temperature.

1. Introduction

The debate about the potential applications of iron-based superconductors is undoubtedly an interesting, still open topic. The properties of these materials, such as very high upper critical fields (H_{c2}) even close to the critical temperature (T_c) and high magnetic field isotropy, make them real competitors of cuprate high temperature superconductors (HTS). Indeed, despite the lower critical temperatures (the highest T_c for this class has been reported to be about 55 K as reported in [1]) compared to those of other HTS, almost all iron-based superconductors are not affected by technical hurdles such as the metal-insulator transition or the d-wave symmetry of the order parameter which can limit their application. Moreover, they also show high robustness to impurities compared to that of cuprate HTS.

Among the different families of iron-based superconductors, one of the most interesting from the point of view of the fabrication of superconducting commercial products such as wires or tapes is that of the iron-chalcogenides (the so-called 11-family). Indeed, they combine the above-mentioned advantageous properties to the peculiar absence of poisonous elements in their chemical formula.

It has been recently demonstrated that it is possible to realize coated conductors based on iron-chalcogenides able to carry very high current densities (critical current densities J_c at 4.2 K and 30 T up to 10^5 A·cm^{-2}) [2] and that it is possible to improve this performance by the right choice of the buffer layer [3, 4, 5]. Moreover, although in several FeSe crystals an high T_c has already reached around 10 K [6], very recently it has been claimed that much higher T_c (from about 80 to 100 K) can been obtained in single layer FeSe [7], making this compound the potential first iron-based "nitrogen" superconductor. On the contrary, these compounds do not appear to provide similar performance in the manufacture of wires [8], but the improvement of the fabrication techniques has led to an enhancement in the current carrying capability of polycrystalline bulk which looks promising in terms of wires production [9, 10]. Although several studies have been performed to elucidate the nature of the superconductivity in Fe-chalcogenides [11, 12], the actual applicative aspects need to be more investigated.

In this paper we will compare the characteristics of samples from different 11-compounds, in particular $FeSe_{1-x}Te_x$ (in the following, FeSeTe) and FeSe, focusing on their pinning properties. Indeed, even if FeSeTe is characterized by higher critical temperature and higher upper critical field slope near T_c, the more simple chemical formula of FeSe could be attractive for wire producers. Thus, our aim is to give a contribution in answering to the question about which compound could be the better choice from the applicative point of view.

2. Experimental details

2.1. Samples preparation

FeSe samples were grown following the NaCl/KCl flux technique developed by Mok et al. [13], with few modifications related to the specifications of the fabrication equipment. In particular, pre-sintered powders of $Fe_{1.02}Se$ and mixture of dried NaCl/KCl (in 1:3 ratio) were sealed in double quartz ampules evacuated to 10^{-3} torr. For the growth procedure a "Carbolite"horizontal tube furnace, with precise temperature control, was used. The quartz ampules were installed tilted at 30°. After an ad-hoc heat treatment similar to the one described in Ref. [13], dozen plate-like FeSe samples with mm-size dimensions were easily separated from the amorphous NaCl/KCl mixture. The final size of the sample is 4 mm × 1 mm, one of the largest obtained [6].

FeSeTe thin films were grown starting from a target of $FeSe_{0.5}Te_{0.5}$ by pulsed laser deposition on CaF_2 substrate. These samples belong to the second generation of high quality and purity thin films, deposited at 550 °C, by a Nd:YAG laser at 1024 nm in place of the KrF at 248 nm wavelength, as previously reported [5]. The FeSeTe samples analyzed in this paper consist of 20 μm width microbridges with a 65 μm distance between the voltage contacts, obtained by standard photolithography [14].

2.2. Compositional analysis

All the samples have been analyzed by Energy Dispersive Spectroscopy (EDS) in order to verify their stoichiometry. Moreover, Electron Backscattered Diffraction (EBSD) has been performed on the FeSe crystals to check the percentage of tetragonal superconductive phase in our sample [6]. EBSD is a surface sensitive technique [28], which is integrated

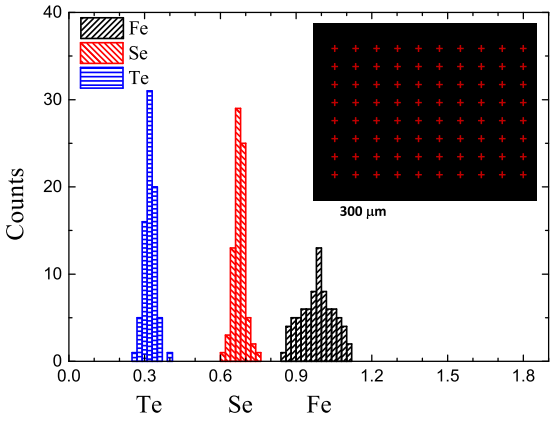

Figure 1. Statistical analysis of a FeSeTe Film. The inset is a SEM image of the sample with a sketch of the grid of points acquired on it.

in our Scanning Electron Microscope (SEM) model LEO EVO50. The orientation distribution of selected regions on the crystals was locally studied by analyzing the signal coming from few tens of nanometers.
Concerning the FeSeTe samples, the starting target was prepared by a two steps procedure from high purity materials (Fe 99.9+%, Se 99.9% and Te 99.999%), with a nominal composition $FeSe_{0.5}Te_{0.5}$ [5]. However the composition study performed on the FeSeTe films has pointed out a Se/Te ratio different from 1.
Grids of about 100 spots of 1 μm of diameter have been acquired on the central area of the samples, each spot being separated from the nearest about 75 μm, with an acquisition time for every spot of 260 s. Figure 1 shows an example of the statistical analysis obtained for each element: the statistical distributions of the data are centered on the element content normalized to the sum of Se and Te. In particular, the following stoichiometry is obtained: $Fe_{0.98}Se_{0.67}Te_{0.33}$, with a root mean square deviation of the same order of that associated with the measure on a single spot (about 5%). The inset of Figure 1 is a sketch of the typical grid of points acquired on one of our samples.
Regarding the FeSe, it is well known that two phases can coexist in this compound: the tetragonal β-phase that is superconducting and slightly Se-deficient, and the hexagonal α-phase that is non superconducting in a wide range of composition, from slightly Fe-rich to Se-rich. It was demonstrated that a suitable thermal treatment allows to reduce the α-phase [13].
Our EDS analysis on the crystals of 11-family compound have shown the following stoichiometry: $Fe_{1.02}Se_{0.98}$. Due to the slightly deficiency of Se, these contents imply that, probably, the majority phase is the β-phase. The EBSD analysis confirms that our crystals contain the two phases and supports the results reported in Ref. [6], in which it is reported a

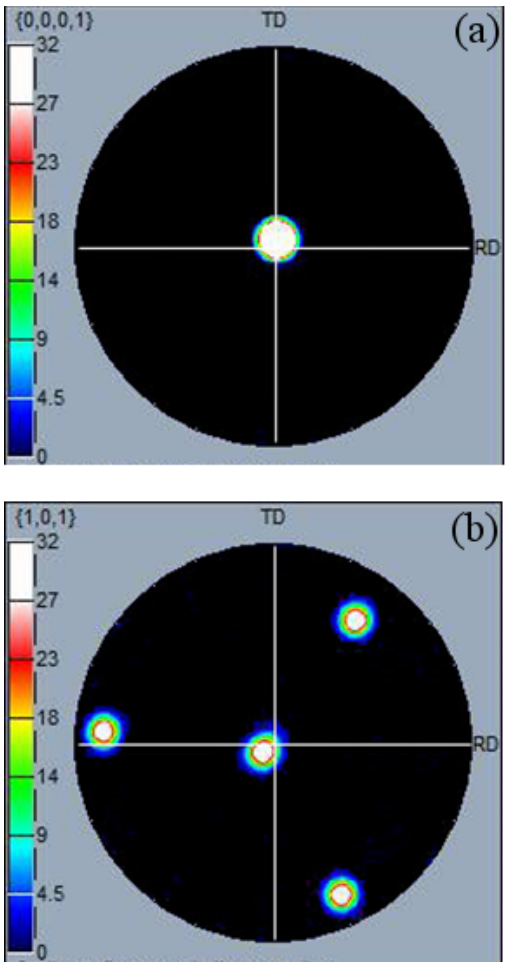

Figure 2. Pole figures obtained by EBSD measurements on FeSe crystals. (a) The pole observed is attributed to the hexagonal α-phase stating the {0001} orientation. (b) It is shown the pole figure related to the β-phase: one orientation, {101}, is observed, slightly drifted with respect to the normal to the sample surface. TD and RD in the pictures indicate the reference transverse and the rolling directions, respectively.

percentage ratio of 82% for the β-phase and 18% for the α-phase. Figure 2 shows the pole figures obtained by measuring several flat areas of the crystals. In particular, panel (a) points out the orientation of the most part of the α-phase along the {0001} direction of the hexagonal crystalline cell. On the contrary, the pole figure of the β-phase in panel (b) shows at least one preferential orientation, along the {101} direction, drifted with respect to the normal to the sample surface ($\theta = 0$, $\phi = 0$) such that $\theta = 6.40°$, $\phi = 124.70°$.

2.3. Experimental setup

The equipment used for DC transport measurements in order to characterize the above-mentioned samples is constituted by: 1) a Cryogen Free Magnet (CFM) system by Cryogenic Ltd. equipped with a cryogen-free variable temperature insert with a base temperature

of 1.6 K and a 9 T superconducting magnet; 2) a Keithley Sourcemeter model 2430 used as bias current source; and 3) a Keithley Nanovoltmeter model 2182 for voltage measurement down to tens of nV. The CFM probe end provides two slots for sample mounting, one for magnetic field orientation perpendicular to the sample surface (H $\perp$), the other for the parallel orientation to the sample surface (H//). The characterization has been carried out through magneto-resistance measurements performed by a standard 4-probe technique and through current-voltage characterizations performed by a pulsed current 4-probe technique (for further details about magneto-resistance and current-voltage measurements, see Ref. [4] and references therein).
Magnetic measurements were performed by means of a Quantum Design PPMS-9T equipped with a VSM option. In particular the relaxation of magnetization as a function of time, as well as DC magnetization curves, were measured at different temperatures (for further details about magnetic measurements, see Ref. [16]).

3. Results and discussion

3.1. Material isotropy

Starting from the analysis of the resistance as a function of the temperature ($R(T)$) curves at several applied magnetic fields, in Figure 3 we show the curves at zero applied magnetic field for both FeSeTe and FeSe samples. From these curves it is possible to estimate the critical temperature applying the standard 50% criterion of normal state resistance (R_N). It results a T_c for the FeSeTe of about 20.5 K, which is well in agreement with that reported in the literature [5, 17]. In the case of the FeSe, the estimation gives a value of about 12.5 K, which is among the highest values registered

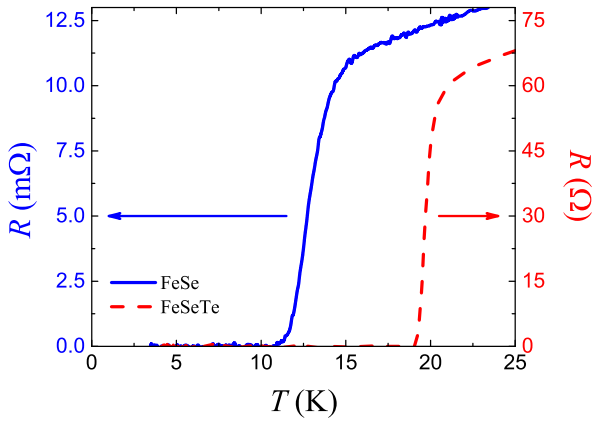

Figure 3. Resistance as a function of the temperature curves at zero applied magnetic field for the two investigated materials.

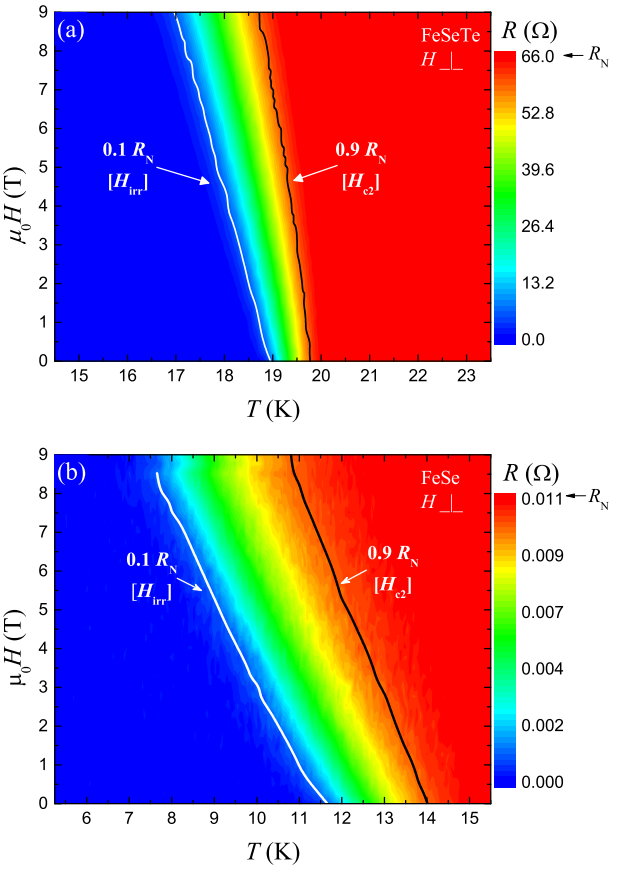

Figure 4. Direct comparison of H-T diagrams for both considered samples. a) The H-T phase diagram of FeSeTe thin film. b) The H-T phase diagram of FeSe sample.

for this compound [9, 11, 12, 18].
Magneto-resistance measurements provide the magnetic field-temperature (H-T) phase-diagrams, as reported in Figure 4 for the two investigated materials. In particular, in Figure 4(a) and (b) the line of irreversibility $H_{irr}(T)$ and the line of the upper critical field $H_{c2}(T)$ are highlighted for the FeSeTe and the FeSe samples, respectively. The two lines have been defined by the standard 90% criterion of R_N for $H_{c2}(T)$, while $H_{irr}(T)$ has been determined by the 10% criterion of the normal state resistance. As it is shown, for the FeSe the superconducting transition width ΔT_c at 0 T is about 2.4 K and at 8 T it is about 3.3 K. Instead, for the FeSeTe $\Delta T_c(0\ \mathrm{T})$ is about 1 K, while it is $\Delta T_c(8\ \mathrm{T})$ about 2.0 K. These results can be interpreted as a clue of the good homogeneity of the samples. From $H_{c2}(T)$ data it is also possible to evaluate the $H_{c2}(T)$ slope near T_c ($\mathrm{d}H_{c2}/\mathrm{d}T|_{T_c}$) for both samples. It results that the $\mathrm{d}H_{c2}/\mathrm{d}T|_{T_c}$ value for the FeSe case is 2.7, which is almost 1/3 than the value obtained for the FeSeTe.
Figure 5 offers a direct way to look at the isotropy of the FeSe sample. In fact, the $H_{irr}(T)$ and $H_{c2}(T)$

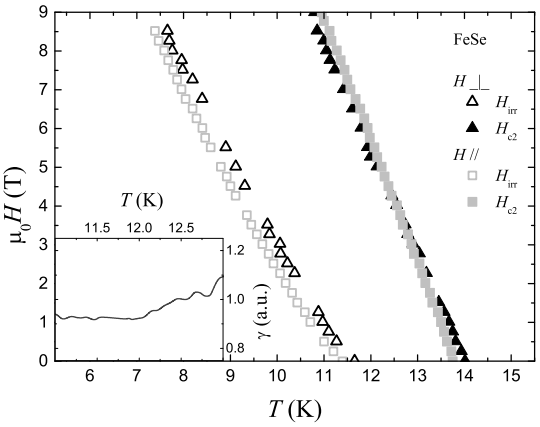

Figure 5. Upper critical field and irreversibility field as a function of the temperature for the FeSe sample. In the inset the anisotropy factor γ as a function of temperature

lines are plotted for the two magnetic field orientations $H \perp$ and $H/\!/$. From these very similar dependences it is quite evident that the superconducting properties of the FeSe are not expected to be strongly influenced by the orientation of the applied magnetic field, as it is the case of the FeSeTe material grown on CaF_2 substrate [14]. This is confirmed by the temperature dependence of the anisotropy factor $\gamma = H^{/\!/}_{c2}/H^{\perp}_{c2}$ that is shown in the inset of Figure 5, which gives an almost constant value around 1 close to T_c, even more isotropic than the FeSeTe thin films usually grown on CaF_2 [14, 19], and the analogous FeSe single crystals [20].

3.2. Pinning properties

The pinning properties of the two investigated compounds have been studied starting from the possible scaling of the normlized pinning force ($f_p = F_p/F_{p,max}$) as a function of the normalized magnetic field ($h = H/H_{irr}$) at different temperatures, as reported in Figure 6. The $f_p(h)$ curves of the FeSeTe sample have been evaluated from current-voltage characteristics, while for the FeSe we refer to the results of magnetic measurements.

In the case of the FeSeTe, it is easier to identify a modified Dew-Hughes scaling law $f_p = w\ C_1\ h^{p_1}(1-h)^{q_1} + (1-w)\ C_2\ h^{p_2}(1-h)^{q_2}$, in which the two components correction is related to the particular nature of their intrinsic pinning centers [5, 14]. In our case, the model curve represented by the solid line in Figure 6(a) can be obtained by fixing $C_1 = 3.49$, $p_1 = 0.5$, $q_1 = 2$ and $C_2 = 6.75$, $p_2 = 1$, $q_2 = 2$. According to the Dew-Hughes model [21], these two components correspond respectively to a 2D δl contribution and to a 1D δl contribution to the overall pinning. The only fitting parameter used is the weight w, whose value results to be $w = 0.66 \pm 0.04$.

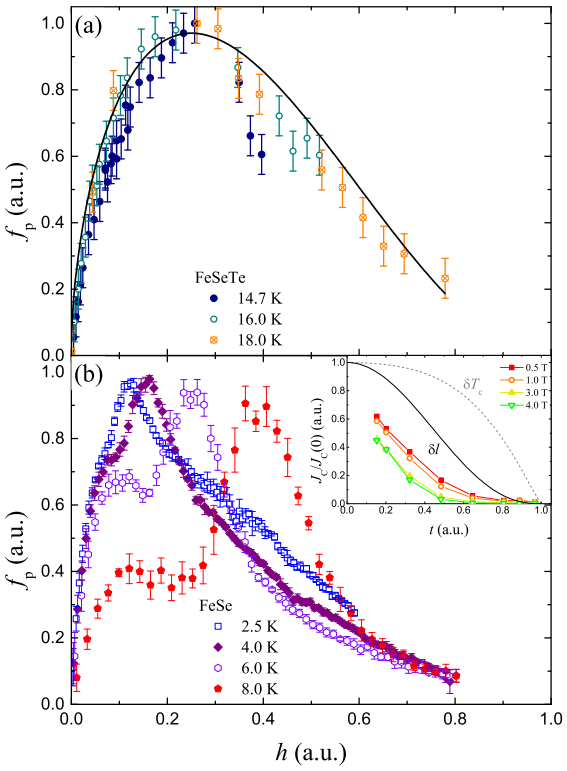

Figure 6. Normalized pinning force as a function of normalized magnetic field: a) for the FeSeTe thin film and b) the FeSe sample at several T. The inset shows the fitting procedure of $J_c(T)$ at several magnetic fields as described in the text.

On the contrary, the FeSe sample shows a quite anomalous behavior both of the shape of the $f_p(h)$ curve and of its temperature dependence. This anomaly reflects the presence of a different pinning mechanism as a function of the temperature, which indeed can be expected due to the multidomain nature of such crystals. In fact it has been recently suggested that this crystal growth results in an aggregate of domains, which contribute both with an interdomain and intergrain critical currents [16]. Thus, the combination of these two contributions does not follows neither the usual Dew-Hughes scaling law $f_p(h)$ [21], nor the modified two components proposed one. Nevertheless, we can recognize an overlap of two different curves, each one with its own peak. The comparison of the behavior in Figure 6(b) with the presence of a multidomain structure in the FeSe sample, which is discussed in detail in Ref. [16], suggests that the fixed low field peak can be related to bulk pinning whereas the higher field peak can be related to domain boundaries. Moreover, we tried to fit the $J_c(T)$ dependence by the standard pinning models δl and δT_c [22], as shown in the inset of Fig-

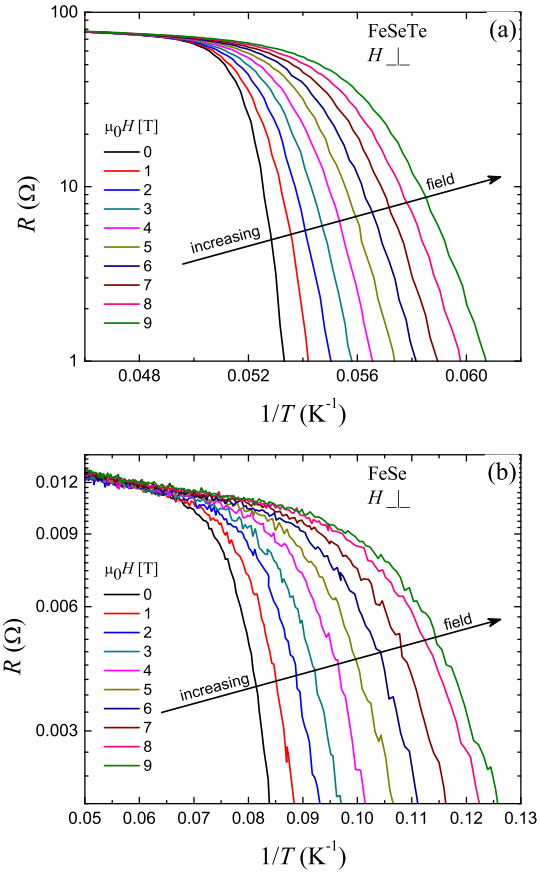

Figure 7. Arrhenius plots at different magnetic fields for both the measured samples: (a) FeSeTe microbridge, (b) FeSe crystal.

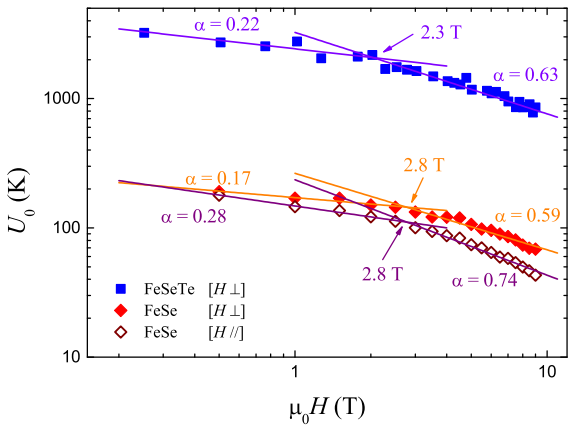

Figure 8. Comparison of the pinning activation energy as a function of the applied magnetic field. The solid lines are fitting lines based on formula $U_0(H) \propto H^{-\alpha}$. The magnetic field is applied perpendicular ($\perp$) and parallel ($/\!/$) to the sample surface.

ure 6(b). Although it is clearly followed the δl-type behavior against the δT_c one, we underline that the only δl contribution is not sufficient to describe the overall pinning. Thus, it should be take into account a more complex variety of pinning centers, which is able to be differently effective as function of the magnetic field as well as the temperature. This is probably the reason why the standard scaling fails and the anomalous "peak effect"appears, as very recently reported [16].

Another important physical quantity that characterizes vortex pinning can be estimated through the analysis of the $R(T)$ curves at different applied magnetic field, and it is the pinning activation energy U. Indeed, in the limit of low current density, the resistance can been written in the form $R(T, H, J) = R_0 \exp[-U(T, H, J)/k_B T]$, where k_B is the Boltzmann constant. Thus, once the current density J is fixed, it is possible to estimate the pinning activation energy curve $U(T, H)$ by the so called Arrhenius plot, obtained by plotting the logarithm of the resistance as a function of the inverse of the temperature (see Figure 7). In this plot, $U(T, H)$ is the slope of the linear region after the onset of the superconducting transition. Following the Tinkham approach [23], the $U(T, H)$ function can be factorized into two contributions $U(T, H) = U_0(H)g(t)$, where $g(t) = (1 - t^2)(1 - t^4)^{1/2}$ (with $t = T/T_c$). In Figure 8 we show the magnetic field contribution $U_0(H)$ to the pinning activation energy. As it is well known, it is $U_0(H) \propto H^{-\alpha}$, where the exponent can assume different values depending on the dominant pinning regime. In particular, when $\alpha \approx 0$ we are dealing with a single vortex pinning regime [24], while for $\alpha > 0.5$ we are in collective-pinning regime [25]. In our case, $U_0(H)$ is almost constant for both FeSeTe and FeSe up to a crossover field value, so we can conclude that vortices in these materials are subject to the action of a strong pinning up to $H = 2.3$ T and 2.8 T, respectively. On the other hand, we have to note that the highest U_0 values are those of FeSeTe, which are a factor 6 higher than those of FeSe in the whole magnetic field range. Nevertheless, this FeSe crystal shows a good isotropy of the pinning energy too, as already stated only for the FeSeTe compound [20], according to the data reported in Figure 5.

In addition, as a standard procedure from relaxation magnetization measurements [26], for the FeSe sample we obtained the temperature dependence of the pinning energy, so that $U(T, H)$ can also be shown in Figure 9. By fitting this temperature behavior at a fixed magnetic field it is possible to determine the n-exponent of the general formula providing the temperature dependence: $g(t) = (1-t^2)^2[(1+t^2)/(1-t^2)]^{n/2}$ [27]. In the inset of Figure 9, the fitting curve is plotted as a continuous (red) line, which is obtained with the n-exponent equal to 3. From this data fitting one should conclude that the right exponent is $n = 3$ at least down to $t = 0.5$, instead of the $n = 1$ usually used in the literature, which is incidentally the exponent we assumed by extracting the data fitting of Figure 8 for

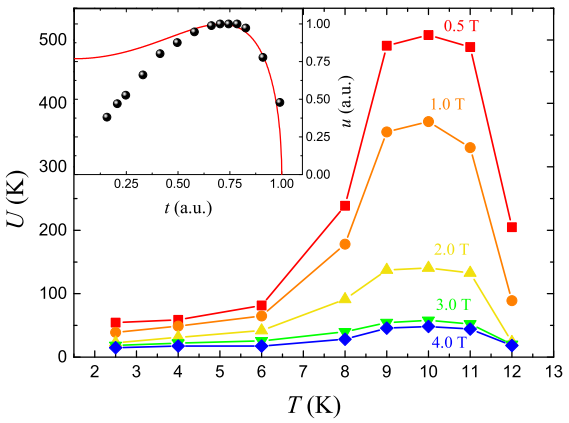

Figure 9. The pinning activation energy as a function of the temperature for different magnetic field values (solid lines are guide for the eye) for the FeSe sample. Inset: The fitting curve explained in the text is displayed together with normalized pinning activation energy $u = U(T, H \to 0)/U_{max}(T, H \to 0)$ data.

the U_0. Therefore, we checked this data fitting by following the generalized formula with $n = 1, 2, 3$ [27], and we realized that the magnetic field dependence of $U(T, H)$ plotted in Figure 8 does not change, while the absolute values can be lowered by a factor of 3 on choosing $n = 3$ instead of $n = 1$. Thus, it is only by measuring the temperature dependence of the pinning energy that it is possible to evaluate the right choice for the n-exponent. The physical meaning of such exponent is related to the relevant length scale for the pinning energy of the flux lines. By selecting $n = 1$ and $n = 3$ the corresponding correlated volume depends on ξ along one or all three directions, respectively. At the end, in the case of FeSe crystals, the overall isotropy observed (see Figures 5 and 8) could justify the choice $n = 3$. If this is the case, a reduction of the pinning energy calculated from the Arrhenius plot is expected, so that the values obtained from direct transport measurements are consistent with the values obtained from magnetic measurements plotted in Figure 9, where a maximum close to the transition is present. Generally, this behavior is associated to a structural transformation of the vortex lattice due to the change of the vortex interaction within a collective pinning model [28, 29, 30, 31].

4. Conclusions

Summarizing, we have shown the results of a comparative analysis on some properties relevant for application of two different compounds (namely FeSeTe and FeSe) belonging to the iron-chalcogenides family of iron-based superconductor. The FeSeTe films of second generation show higher critical temperature, higher upper critical field slope near T_c and higher pinning activation energies compared to those of FeSe crystals. By the way, the magnetic field dependence of the pinning energy $U(T, H) = U_0(H)g(t)$ derived from direct transport measurements depends on the choice of the n-exponent of the $g(t)$. Therefore the absolute values usually obtained from direct transport measurements are overestimated with respect to the values obtained by magnetization measurements. Anyway, both the resistive and magnetisation experiments have revealed highly unusual and diverse pinning behaviour of the FeSe crystals, unexplored so far, probably determined and influenced by their complex multidomain structure.

Thus, our conclusion is that chalcogenide compounds can offer the great advantage of high isotropic pinning properties, and this can be achieved with a proper choice of the substrate, that is CaF_2 for the FeSeTe films, and an optimized growth procedure for the FeSe bulk material.

Acknowledgments

Authors thank A. Vecchione for useful discussion on EBSD analysis.
A.L. and A.G. acknowledges financial support from PON Ricerca e Competitivitá 2007-2013 under Grant Agreement PON NAFASSY, PONa3_00007. This work was also financially supported by the inter-academic Italian-Bulgarian research project (Physics Department "E.R. Caianiello" CNR-SPIN unit, Salerno University and Solid State Physics Institute "Georgy Nadjakov", Bulgarian Academy of Sciences).

References

[1] Tanabe K and Hosono H 2011 Frontiers of Research on Iron-Based Superconductors toward Their Application *Japan. J. Appl. Phys.* **51** 010005.
[2] Si W, Han S J, Shi X, Ehrlich S N, Jaroszynski J, Goyal A and Li Q 2013 High current superconductivity in $FeSe_{0.5}Te_{0.5}$-coated conductors at 30 tesla *Nature Communication* **4** 1347.
[3] Kawale S, Bellingeri E, Braccini V, Pallecchi I, Putti M, Grimaldi G, Leo A, Guarino A, Nigro A and Ferdeghini C 2013 Comparison of Superconducting Properties of $FeSe_{0.5}Te_{0.5}$ Thin Films Grown on Different Substrates *IEEE Trans. Appl. Supercond.* **23** 7500704.
[4] Leo A, Guarino A, Grimaldi G, Nigro A, Pace S, Bellingeri E, Kawale S, Ferdeghini C and Giannini E 2014 Comparison of the pinning energy in $Fe(Se_{1-x}Te_x)$ compound between single crystals and thin films *J. Phys.: Conf. Ser.* **507** 2014 012029.
[5] Bellingeri E *et al* 2014 High field vortex phase diagram of Fe(Se, Te) thin films *Supercond. Sci. Technol.* **27** 044007.
[6] Buchkov K *et al* 2015 Investigation of the vortex dynamics of $Fe_{1.02}Se$ crystals by fundamental and 3rd harmonic ac magnetic susceptibility analysis *Supercond. Sci. Technol.* **28** 035009
[7] Ge J-F, Liu Z-L, Liu C, Gao C-L, Qian D, Xue Q-K, Liu Y and Jia J-F 2015 Superconductivity above 100 K in

single-layer FeSe films on doped $SrTiO_3$ *Nat. Mater.* **14** 285-289.
[8] Ma Y 2012 Progress in wire fabrication of iron-based superconductors *Supercond. Sci. Technol.* **25** 113001.
[9] Wu M K, Wang M J and Yeh K W 2013 Recent advances in β-$FeSe_{1-x}$ and related superconductors *Sci. Technol. Adv. Mater.* **14** 014402.
[10] Palombo M, Malagoli A, Pani M, Bernini C, Manfrinetti P, Palenzona A and Putti M 2015 Exploring the feasibility of Fe(Se,Te) conductors by ex-situ powder-in-tube method *J. Appl. Phys.* **117** 213903.
[11] Chang C C, Chen T K, Lee W C, Lin P H, Wang M J, Wen Y C, Wu P M and Wu M K 2015 Superconductivity in Fe-chalcogenides *Physica C* **514** 423-434.
[12] Hosono H and Kuroki K 2015 Iron-based superconductors: Current status of materials and pairing mechanism *Physica C* **514** 399-422.
[13] Mok B *et al* 2009 Growth and Investigation of Crystals of the New Superconductor β-FeSe from KCl Solutions *Crystal Growth & Design* **9** 3260-3264.
[14] Braccini V *et al* 2013 Highly effective and isotropic pinning in epitaxial Fe(Se,Te) thin films grown on CaF_2 substrates *Appl. Phys. Lett.* **103** 172601.
[15] Schwartz A J, Kumar M, Adams B L 2000 Electron Backscattered Diffraction in Material Science, (New York: Kluwer Academc-Plenum Publisher).
[16] Galluzzi A *et al* 2015 Evaluation of the intragrain critical current density in a multidomain FeSe crystal by means of DC magnetic measurements *accepted for pubblication in Supercond. Sci. Technol.*.
[17] Bellingeri E *et al* 2010 T_C = 21 K in epitaxial $FeSeB_{0.5}Te_{0.5}$ thin films with biaxial compressive strain *Appl. Phys. Lett.* **96** 102512
[18] Ma M W, Yuan D N, Wu Y, Dong X L and Zhou F 2014 Crystal growth of iron-based superconductor $FeSe_{0.94}$ by KCl flux method *Physica C* **506** 154157.
[19] Yuan P *et al* 2015 High performance $FeSe_{0.5}Te_{0.5}$ thin films grown at low temperature by pulsed laser deposition *Supercond. Sci. Technol.* **28** 065009.
[20] Her J L *et al* 2015 Anisotropy in the upper critical field of FeSe and $FeSe_{0.33}Te_{0.67}$ single crystals *Supercond. Sci. Technol.* **28** 045013.
[21] Dew-Hughes D 1974 Flux pinning mechanisms in type II superconductors *Phil. Mag.* **30** 293.
[22] Bonura M, Giannini E, Viennois R and Senatore C 2012 Temperature and time scaling of the peak-effect vortex configuration in $FeTe_{0.7}Se_{0.3}$ *Phys. Rev. B* **85** 134532.
[23] Tinkham M 1988 Resistive Transition of High-Temperature Superconductors *Phys. Rev. Lett.* **61** 1658-1661.
[24] Blatter G, Feigel'man M V, Geshkenbein V B, Larkin A I and Vinokur V M 1994 Vortices in high-temperature superconductors *Rev. Mod. Phys.* **66** 1125-1338.
[25] Yeshurun Y and Malozemoff A P 1998 Giant Flux Creep and Irreversibility in an Y-Ba-Cu-O Crystal: An Alternative to the Superconducting-Glass Model *Phys. Rev. Lett.* **60** 2202-2205.
[26] Lan M D, Liu J Z and Shelton R N 1991 Flux creep in iron-doped Y-Ba-Cu-O single crystals *Phys. Rev. B* **44** 2751-2756.
[27] Budhani R C, Welch D O, Suenaga M and Sabatini R L 1990 Field-Induced Broadening of the resistive Transition and Two-Dimensional Nature of Flux Pinning in $Y_2Ba_4Cu_8O_{16}$ Films *Phys. Rev. Lett.* **64** 1666-1669.
[28] Miu D, Noji T, Adachi T, Koike Y and Miu L 2012 On the nature of the second magnetization peak in $FeSe_{1-x}Te_x$ single crystals *Supercond. Sci. Technol.* **25** 115009.
[29] Pramanik A K, Harnagea L, Nacke C, Wolter A U B, Wurmehl S, Kataev V and Büchner B 2011 Fishtail effect and vortex dynamics in LiFeAs single crystals *Phys. Rev. B* **83** 094502.
[30] D. Botta *et al.* 2002 Temperature, field and current dependence of the flux creep activation energy in bulk MgB_2 *Physica C* **369** 232-235.
[31] T. Matsushita 1993 On the flux bundle size in weakly pinned superconductors *Physica C* **217** 461-466.